Down-Flow Shell-Side Forced Convective Boiling

One hundred sets of R-11 two-phase pressure drop and boiling heat transfer data are reported for cocurrent down-flow over an in-line tube bundle. The pressure drop data agree with predictions using the Diehl correlation. A new heat transfer correlation is reported, accounting for the observed convective and nucleate mechanisms.

D. L. Bennett, B. L. Hertzler, C. E. Kalb
Process Systems Group
Air Products and Chemicals, Inc.
Allentown, PA 18105

SCOPE

Down-flow evaporation can result in very effective heat transfer due to gravity thinning of the liquid film. The heat transfer and pressure drop characteristics must be predicted accurately during the design stage of a heat exchanger to properly determine the thermal driving force and size of the heat exchanger. An objective of this paper is to present experimental pressure drop and heat transfer coefficient data over a reasonable range of mass flux and a large range of vapor quality and heat flux. These data will illustrate whether down-flow shell-side boiling exhibits the same characteristics exhibited by tube-side boiling. An additional objective is to develop a mechanistic correlation for the heat transfer coefficient. This correlation will be useful in the design of process heat exchangers with shell-side evaporation.

CONCLUSIONS AND SIGNIFICANCE

One hundred sets of R-11 two-phase pressure drop and heat transfer data are reported for down-flow, shell-side forced convective boiling. The experimental apparatus and methods to account for angular variations in the heat transfer coefficient are described.

The Diehl (1957) correlation for two-phase pressure drop successfully predicts the variation in pressure drop with quality. The heat transfer results indicate that:

1. For low values of wall superheat, ΔT_s, the heat transfer coefficient is insensitive to wall superheat. In this range of wall superheats, the heat transfer appears to be controlled by the convective boiling mechanism.
2. In the convective-dominated region, the heat transfer coefficient is insensitive to mass flux.
3. In the convective-dominated region, for constant values of liquid mass flux, increasing the vapor flux significantly increases the heat transfer coefficients.
4. At higher values of wall superheat, the forced convective boiling heat transfer coefficients approach the pool boiling heat transfer coefficients.
5. The additional heat transfer attributable to nucleate boiling is suppressed at higher values of mass flux.

With the exception of point 2, these trends are similar to those seen for tube-side flow. Since tube-side flow is successfully correlated by additive approaches such as that of Chen (1966), a heat transfer correlation using additive mechanisms was developed from these data.

The Bays and McAdams (1937) correlation for viscous flow over tubes is used as a basis for the convective heat transfer coefficient. Analysis shows that the magnitude of the observed increase in the convective coefficient resulting from an increase in vapor flux cannot be explained by shear thinning of the liquid film. The

Correspondence concerning this paper should be addressed to D. L. Bennett.
C. F. Kalb is now with Grumman Aerospace Corporation, Bethpage, New York.

observed increase is attributed to entrainment, and a correlation is developed that predicts the apparent entrainment vs. a parameter similar to that proposed by Wallis (1968). The method proposed by Bennett et al. (1980) is used successfully to predict the nucleate boiling contribution to the overall heat transfer coefficient.

The correlation for the heat transfer coefficient, accounting for both the nucleate and convective mechanisms, collapses the heat transfer data to give a mean error of 9.5% and an average error of 0.5%. The correlation is expected to be reasonable for upward vapor flow in addition to downward vapor flow.

Experimental

R-11 (Freon 11, CCL_3F) was selected as the test fluid since its normal boiling point is near ambient temperatures. The ratio of several liquid properties to the properties of ambient temperature water are, ρ_L:1.48, μ_L:0.47, k_L:0.17. The vapor density of R-11 at normal boiling point is 5.84 kg/m^3.

Figure 1 is a schematic flowsheet of the R-11 test loop. An electrically heated reboiler supplies vapor to the test section, and liquid is pumped to the test section from the bottom of the reboiler. Vapor and liquid flow rates are measured with an Annubar flowmeter and rotameter, respectively. The vapor quality based on flowmeter readings is corrected for possible subcooling or superheating of either feed relative to the equilibrium mixed temperature in the test section. This correction to the vapor quality is derived from an enthalpy balance on the test section and is always small. The two-phase R-11 stream flows downward through the test section and into a separator vessel. The vapor phase is then condensed and returned to the separator. The pressure level in the test loop is slightly above ambient pressure and is controlled automatically by regulating the flow rate of cooling water to the condenser. Liquid R-11 is then recirculated from the separator vessel to the reboiler.

Figure 2 illustrates the test section. The test section was constructed primarily of brass and copper and had a clear polycarbonate front face plate (*1*) for viewing. The tube bundle (*2*) was made from 9.52 mm OD aluminum bars (*3*) and comprised eight tube rows and three tube layers, with half-bars (*4*) on the walls in an in-line square-pitch arrangement. The internal dimensions of the test section are 127 mm wide by 380 mm high. The ratio of tube pitch to tube diameter is 1.24.

The vapor entering the test section is distributed by a sintered metal plate. Liquid enters through a concentric double-tube distributor (*5*) and is directed vertically upward into the oncoming vapor. The outer tube (9.52 mm OD) and inner tube (6.35 mm OD) of this distributor both have 18 equally spaced holes, respectively 1.15 and 1.00 mm in diameter. The first five rows of the tube bundle serve as a two-phase distributor to further ensure representative flow distribution at the sixth tube row, where heat transfer measurements are made.

The instrumented test element (*6*) in the sixth tube row is inserted through ports in the side of the test section. This single active element can be rotated to various angular positions so that the wall temperature can be averaged at many points around its periphery. To test whether the single heated tube is sufficient to obtain heat transfer coefficients representative of those seen in a heated tube bundle, additional tests were carried out. With representative two-phase flow conditions, two additional tube rows were heated (at the same heat flux) immediately upstream of the test element. Under these conditions, the heat transfer coefficient was reevaluated and found to be between 2 and 4% less than observed when only the single tube was heated. Therefore, the heat transfer coefficients in an actual heat exchanger are expected to be lower than the data reported here by no more than this amount.

The active test element was 102 mm long and was machined from aluminum bar stock. A hole was drilled the full length of the test element to accommodate a cartridge heater made by wrapping nichrome wire around an alumina mandrel. The uniform windings were covered with a ceramic cement, and the small void space between the cartridge heater and the inside of the test element was filled with a heat transfer compound. A

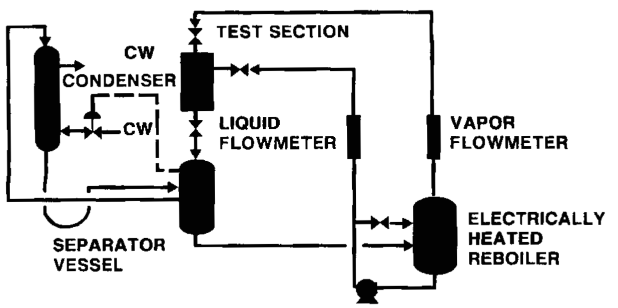

Figure 1. Two-phase R-11 shell-side heat transfer loop.

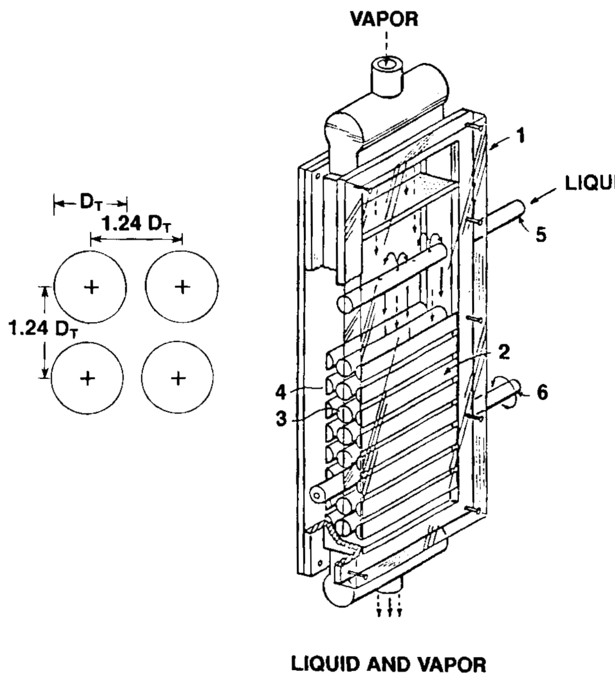

Figure 2. Test section.

short (6.35 mm) length of Teflon bar of the same diameter as the test element was attached to each end of the heated test element for support and thermal insulation. End heat losses were evaluated analytically and found to be insignificant.

The generally small temperature differences typical of efficient evaporation processes place special emphasis on the accuracy of the temperature measurements required to determine the heat transfer coefficients. An opposed thermopile circuit was used to measure directly the temperature difference between a known point within the wall of the test element and the bulk fluid. One of the two thermopiles was located within a small hole 51 mm deep drilled longitudinally in the wall of the heated test element; the other thermopile was embedded within the unheated half-bar on the back wall of the test section, immediately adjacent to the test element. This latter thermopile sensed the bulk fluid temperature. The average temperature at the test element thermopile was determined by taking readings of the opposed thermopile circuit output at as many as 13 different angular positions around the periphery of the test element. The resulting average interior wall temperature at the thermopile hole radius was then corrected, assuming one-dimensional, radial conduction, to give the average surface temperature. The exact radial position of the wall thermopile hole was determined by sectioning the test element at the bottom of the hole after the heat transfer tests were completed. A more detailed two-dimensional least-squares analysis which used the local wall temperature measurements and an assumed quartic polynomial distribution for the surface temperature gave average heat transfer coefficients that were within 0.1% of those calculated from the simple one-dimensional analysis.

The individual type K thermocouples in the thermopiles were stainless steel-sheathed (0.254 mm OD) with ungrounded junctions and were made from a single lot of wire. Five thermocouples were used in each thermopile to amplify the circuit output to improve accuracy. Each of the reference junctions of the thermocouples was sealed in a glass tube filled with mineral oil. These glass tubes were then placed in holes drilled in a large block of brass and immersed in a constant-temperature bath. The temperature of this bath is immaterial to the measurement.

The electric signal from the opposed thermopile circuit must first be corrected by subtracting the zero-offset reading obtained with no power supplied to the test element cartridge heater. This correction was generally very small. Dividing the resulting EMF by the number of thermocouples in each thermopile and by the thermoelectric power (e.g., mv/°C) of the thermocouple pair used gives the temperature difference between the thermopiles. The thermoelectric power is evaluated iteratively at the average temperature of the two thermopiles, using standard thermocouple data. Special tests using various known temperature differences gave accuracies of 0.2% or better for this technique. R-11 vapor heat transfer coefficients measured using this technique were within a few percent of the Grimison (1937) correlation for single-phase heat transfer.

Pressure taps before and after the tube bundle were used to measure the tube bundle pressure drop. Lines from these taps were led upward to 1 L surge vessels in a heated water bath. The surge vessels provided a capacitance in the pressure tap lines, which was effective in damping the fluctuating pressures typical of two-phase flow. The heated water baths prevented condensation of R-11 in the surge vessels. The pressure difference between the surge vessels was then measured using a differential pressure transducer.

Results

Tests were carried out at four values of the total mass flux, approximately 102,000, 193,000, 284,000, and 377,000 kg/h · m^2, and at qualities at the instrumented tube of approximately 0, 25, 50, 70, and 90% vapor. For all data, the test section pressure ranged from 1.0 to 1.07 atm, with over 50% of the runs ranging from 1.03 to 1.05 atm. At each flow condition, measurements were made at five values of heat flux. For the entire set of data, the heat flux varied between 2,000 and 94,000 W/m^2, resulting in a wall superheat range from 1.3 to 13°C. This range was selected to allow measurements in both the convective-dominated boiling regime and under conditions where nucleate boiling contributes significantly to the overall heat transfer. The resulting heat transfer coefficients ranged from 1,300 to 7,300 W/m^2 · C.

In Figure 3, the experimental two-phase pressure drop is plotted vs. quality for the tested range of mass flux. No variation in the pressure drop was observed as the wall superheat was changed. Furthermore, the pressure drop at zero vapor flow was measured and found to be negligible at all liquid rates. The pressure drop was also measured under all vapor flow conditions. An empirical fit of these data is,

$$\Delta P_{VT} = 4 f_{VT} \frac{\rho_V V_{VT\max}^2}{2 g_c} \tag{1a}$$

where

$$f_{VT} = 0.72\, \mathrm{Re}_{VT}^{-0.22}. \tag{1b}$$

The two-phase data indicate that at a given quality, the pressure drop per tube row is approximately proportional to the mass flux squared.

In Figure 4, the experimental heat transfer coefficients are plotted vs. wall superheat (ΔT_s) for the ranges of mass fluxes and qualities tested. For reference, the experimentally evaluated pool boiling curve (the thicker curve) is also given. This curve was obtained by flooding the test chamber with R-11. The following general trends are seen:

1. Many of the data exhibit a classical convective-dominated boiling region. This region occurs for these test conditions at a wall superheat less than about 7°C.

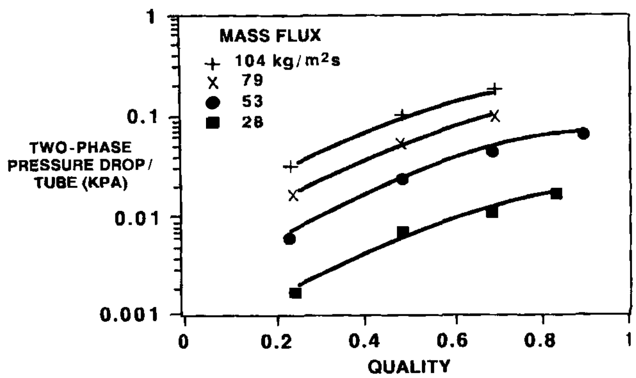

Figure 3. Pressure drop/tube vs. quality.

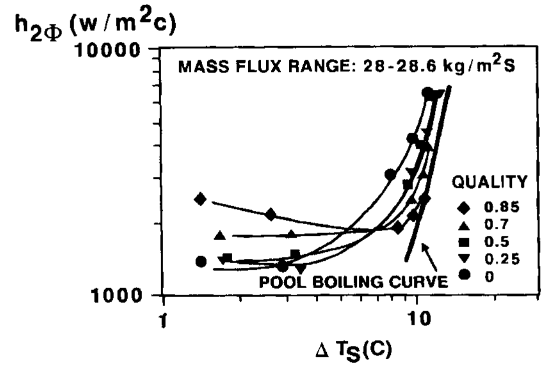

Figure 4A. $h_{2\phi}$ **vs. wall superheat** ΔT_s.

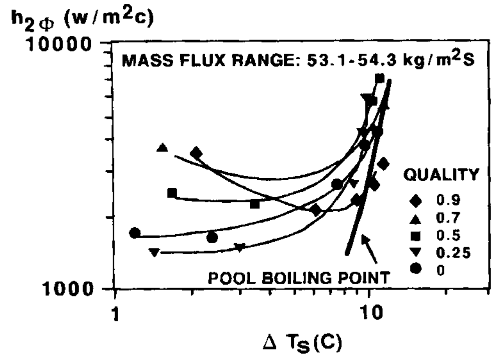

Figure 4B. $h_{2\phi}$ **vs. wall superheat** ΔT_s.

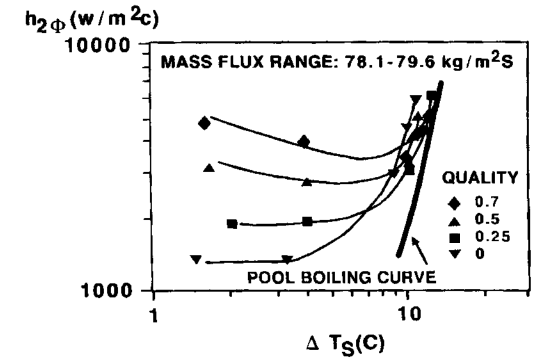

Figure 4C. $h_{2\phi}$ **vs. wall superheat** ΔT_s.

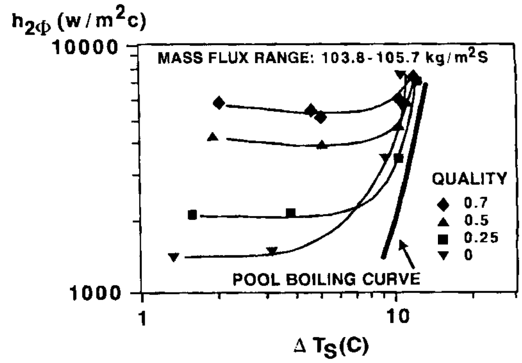

Figure 4D. $h_{2\phi}$ **vs. wall superheat** ΔT_s.

2. In the convective-dominated boiling region, the data taken at qualities of 85% and greater exhibit a gradual decrease in heat transfer coefficient as ΔT_s increases. Since this is an unexpected result, data in this region were rechecked and analyzed for any possible systematic errors. The authors are convinced that this phenomenon is real for this geometry. At higher wall superheat, the coefficient increases as nucleate boiling becomes more significant.

3. In the convective-dominated boiling region, the heat transfer coefficient is not sensitive to total mass flux at low values of vapor flux.

4. At test conditions with constant values of liquid mass flux $[G(1 - x)]$, an increase in vapor flux significantly increases the heat transfer coefficients.

5. The pool boiling heat transfer coefficient increases sharply with increasing superheat.

6. The forced convective boiling data with superheat greater than about 8°C tend to approach the pool boiling curve and exhibit a dependency on ΔT_s similar to the pool boiling curve.

7. At high values of mass flux, the nucleate boiling contribution to the overall coefficient appears to be less than the contribution at lower values of mass flux, for equal values of ΔT_s.

Correlation Development

Pressure drop per tube

For down-flow, thin-film boiling on tube banks, the continuous phase is the vapor phase. Therefore, it is reasonable to normalize the two-phase pressure drop by a pressure drop for vapor flow. Typically, either the pressure drop calculated using the entire flow as vapor (ΔP_{VT}) or the vapor-only pressure drop ($\Delta P_{V_{only}}$) would be selected. Diehl (1957) chose to normalize the two-phase pressure drop by the pressure drop calculated using the entire flow as vapor (ΔP_{VT}).

These experimental data are normalized by ΔP_{VT}, which is calculated from Eqs. 1a and 1b. In Figure 5, the ratios are plotted vs. the Diehl parameter, $(1 - \alpha s)/[(\rho_V/\rho_L)Re_{VT}^{0.2}]$. Also plotted is the curve recommended by Diehl. Agreement is reasonable, and if the curve recommended by Diehl is used in conjunction with the empirically derived expression for ΔP_{VT}, the

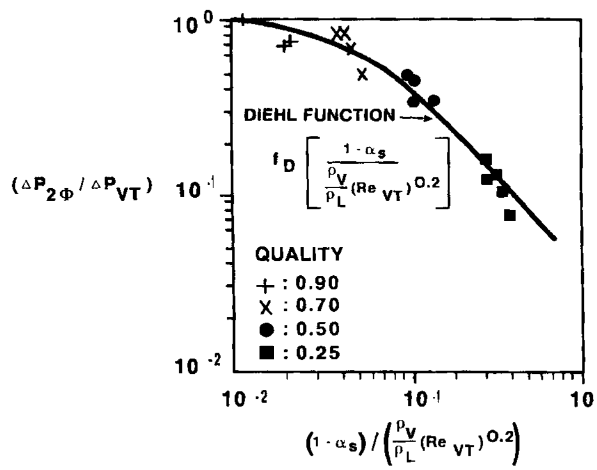

Figure 5. Normalized two-phase pressure drop per tube vs. Diehl parameter.

two-phase pressure drop data are correlated to within an average error of +9% and a mean error of 15%. (Average error = Σ % error/number of data points. Mean error = Σ |% error|/number of data points.) This success is consistent with the conclusions made by Ishihara et al. (1980).

Heat transfer coefficient

As described earlier, the heat transfer coefficients reported in Figure 4 show many of the classic phenomena exhibited by two-phase tube-side flow data. Major examples are a convectively dominated region, and a nucleate-dominated region that exhibits suppression of the nucleate mechanism at higher values of mass flux. Based on the success of additive heat transfer mechanism correlations for tube-side flow to account for these phenomena, the following correlation format is assumed for thin-film shell-side boiling: $h_{2\phi} = h_{conv} + \overline{h}_{NUC}$, where h_{conv} is the convective-dominated boiling heat transfer coefficient and $\overline{h}_{NUC}$ is the contribution resulting from nucleate boiling. The correlation for h_{conv} is developed from a liquid-only coefficient, h_g, and a multiplier that accounts for the increase in the heat transfer coefficient with increasing vapor flux.

For single-phase flow over a tube bank, Bays and McAdams (1937) recommended a correlation for h_g which, using the definition for G, can be modified to the following:

$$h_g = C_1\left(\frac{2k_L^2\rho_L^{4/3}g^{2/3}C_{PL}}{\pi D_T\mu_L^{1/3}}\right)^{1/3}\left(\frac{\mu_L}{\mu_w}\right)^{1/4}\left[\frac{2G(1-x)\,S_w}{\mu_L}\right]^{1/9} \tag{2}$$

Bays and McAdams recommended that C_1 equal 0.672. The last group in brackets is identical to the liquid-only Reynolds number, $4\,\Gamma/\mu_L$. For this set of data, $4\,\Gamma/\mu_L$ ranges from 40 to 1,000, which is well below the limit of 2,100 recommended by Bays and McAdams. Equation 2 predicts a very weak dependency of h_g on mass flux, G. Figure 4 shows that the zero quality data taken for this study demonstrate a very weak dependency on mass flux. This is consistent with the Bays and McAdams correlation. Based on data analysis discussed later, a value of 0.886 for C_1 will be recommended.

Equation 2 also predicts a very weak dependency on quality. However, as seen in Figure 4, at test conditions with equal values of liquid mass flux, the heat transfer coefficient in the convective-dominant boiling region is a strong function of the quality. At constant mass flux, increasing the quality decreases the liquid-only Reynolds number, $4\,\Gamma/\mu_L$. Therefore, it is unlikely that the enhancement is due to an increase in the turbulence in the liquid film. Since the heat transfer resistance is across the liquid film, and the film is probably laminar, a possible mechanism for decreasing the resistance is a thinning of the liquid film. Film thinning can result as vapor flux increases by shear thinning of the film and/or entrainment of the liquid into the vapor core.

If we assume laminar flow in the film, and use a force balance that includes forces due to wall shear stress, gravity, and interfacial shear stress, the influence of vapor shear on the film thickness can be estimated for an assumed value of interfacial shear stress. Even if we use the maximum possible interfacial shear stress corresponding to the entire two-phase pressure drop gradient, the film thickness is calculated to thin by less than 10% for all test conditions. Therefore, if the film is assumed to be laminar, shear thinning should not significantly increase the convective portion of the total heat transfer coefficient. However, if we compare the convective-dominated 0.50 quality, 377,000 kg/h · m² mass flux heat transfer coefficients to those of the zero quality data at 193,000 kg/h · m², a factor of about three exists between the coefficients despite comparable liquid fluxes.

A possible mechanism to explain the increase in the heat transfer coefficient as the vapor flux increases is entrainment of a portion of the liquid film into the vapor. If we assume that the temperature profile in the film approaches a fully developed linear profile, the following relationship would be expected,

$$\frac{\delta_{conv}}{\delta_g} = \frac{h_g}{h_{conv}} \tag{3}$$

Although this assumption is not strictly correct due to the thermal entry length near the top of each tube, it will be made to simplify the following analysis.

For fully developed laminar flow in a film, the thickness of the film is proportional to the liquid mass flow raised to the ⅓ power. Using this plus Eq. 3 gives,

$$\frac{h_{conv}}{h_g} = (1-\epsilon)^{-1/3} \tag{4a}$$

or,

$$\epsilon = 1 - \left(\frac{h_g}{h_{conv}}\right)^3 \tag{4b}$$

where ϵ is the apparent mass fraction of liquid entrained in the vapor.

Our intention is to use Eq. 4 to determine from the experimental data values for ϵ. Wallis (1968) has proposed that ϵ is a function of a parameter, π_1, where,

$$\pi_1 = \frac{V_{V\max}\mu_v}{\sigma g_c}\left(\frac{\rho_V}{\rho_L}\right)^{1/2} \tag{5a}$$

If we assume that the two-phase pressure drop obeys

$$\Delta P_{2\phi} = K_{2\phi}\rho_v\frac{V_{V\max}^2}{2gc}$$

where $K_{2\phi}$ is a two-phase velocity head loss coefficient, then an alternate expression to Eq. 5a is

$$\pi_2 = \left(\frac{\Delta P_{2\phi}}{g_c\rho_L}\right)^{1/2}\frac{\mu_v}{\sigma} \tag{5b}$$

Since π_2 would vary as a function of tube layout, π_2 may be more appropriate than π_1 for shell-side two-phase flow.

Figures 6A and 6B give plots of the apparent values for ϵ, determined from Eq. 4b, vs. π_1 and π_2. Only data that were dominated by the convective heat transfer mechanism were used to generate these plots. C_1 was given a value of 0.886 for this regression. The curve fits obtained are,

$$\epsilon = 1 - \exp(0.23 - 10{,}200\,\pi_1)$$

$$\epsilon = 1 - \exp(0.26 - 24{,}000\,\pi_2)$$

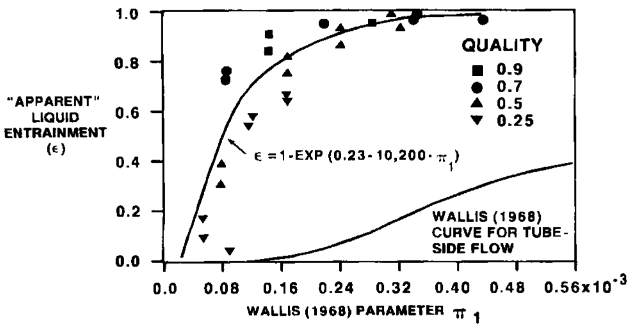

Figure 6A. Apparent entrainment vs. π_1.

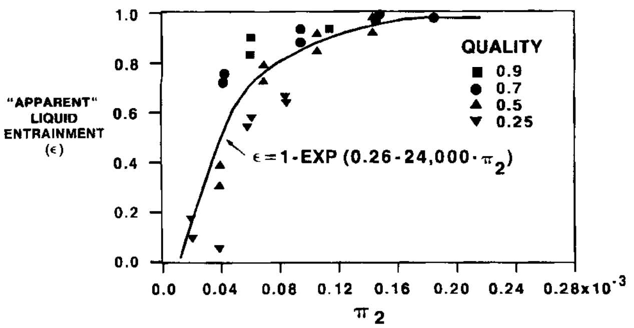

Figure 6B. Apparent entrainment vs. π_2.

(For values of π_1 or π_2 that result in ϵ being less than zero, ϵ should be set equal to zero.)

Figure 6A also gives the Wallis curve for tube-side flow. The apparent entrainment is significantly greater at a given value of $V_{V\max}$ than that which would be expected for tube-side flow. However, this trend is reasonable since at comparable values of $V_{V\max}$ the pressure drop across a tube row is substantially greater than the pressure drop in a tube with a length equal to the tube diameter. Even though this trend is reasonable, it must be recognized that ϵ may not represent the actual entrainment. The use of an apparent entrainment simply allows us to identify a reasonable correlation parameter, i.e., π_2. Test data for another system would allow a test of the adequacy of this grouping.

Correlation for $\bar{h}_{NUC}$

The method proposed by Bennett et al. (1980) was used to predict the contribution to the heat transfer resulting from nucleate boiling. Their method accounts for the suppression of nucleate boiling by convective flow. The approach has the following three steps:

1. Identify the pool boiling correlation most valid for the fluid, tube material, pressure, and wall superheat range desired.
2. Reformulate the pool boiling correlation so that the pool boiling coefficient can be directly related to the wall superheat, ΔT_s, and physical properties.
3. To account for the influence of convective flow, substitute $S\Delta T_s$ for ΔT_s.

The expression for S is based on an analytical development that includes calculation of the average superheat. This procedure accounts for the temperature variation in the liquid near the heated wall, over a growth region X_o. Their expression is

$$S = \frac{k_L}{h_{conv}X_o}\left(1 - \exp - \frac{h_{conv}X_o}{k_L}\right)$$

where

$$X_o = 0.041\left[\frac{g_c\sigma}{g(\rho_L - \rho_V)}\right]^{1/2}$$

For this study, the correlation of Borishanskiy et al. (1963) for pool boiling is selected as the basis for the nucleate boiling contribution. Their correlation is,

$$Nu_B = 8.7 \times 10^{-4} Pe^{0.7} K_P^{0.7}$$

where

$$Nu_B = \frac{\bar{h}_{PB}}{k_L}\left[\frac{g_c\sigma}{g(\rho_L - \rho_V)}\right)^{1/2}$$

$$Pe = \frac{\rho_L}{\rho_V}\frac{\bar{h}_{PB}\,\Delta T_s}{\mu_L h_{fg}}\left(\frac{g_c\sigma}{g(\rho_L - \rho_V)}\right)^{1/2}\frac{\mu_L C_{PL}}{k_L}$$

$$K_P = \frac{P}{\left[\dfrac{g\sigma(\rho_L - \rho_v)}{g_c}\right]^{1/2}}$$

Pool boiling data reported by Kadi (1975) and Chou (1975) used this correlation but recommended that Pe be raised to the approximately 0.8 power instead of 0.7. The format of the pool boiling correlation assumed for this shell-side study is: $Nu_{NUC} = C_2 Pe_*^n K_P^{0.7}$, where Nu_{NUC} is identical to Nu_B except that $\bar{h}_{NUC}$ replaced $\bar{h}_{PB}$. Furthermore, C_2 replaces 8.7×10^{-4} to account for differences in the surface roughness of the heated tube and to account for circumferential variations in the tube wall temperature. Pe_* replaces Pe as recommended by Bennett et al. (1980), where Pe_* is defined by,

$$Pe_* = \frac{\rho_L}{\rho_V}\frac{\bar{h}_{NUC}S\Delta T_s}{\mu_L h_{fg}}\left(\frac{g_c\sigma}{g(\rho_L - \rho_V)}\right)^{1/2}\frac{\mu_L C_{PL}}{k_L}$$

The entire set of experimental data was analyzed to evaluate C_2 and n. The contribution resulting from nucleate boiling was evaluated by subtracting h_{conv} from $h_{2\phi}$; in addition to determining values for C_2 and n, C_1 as defined in Eq. 2 was also experimentally evaluated. The resulting constants are:

$$C_1 = 0.886$$

$$C_2 = 8.0 \times 10^{-4}$$

$$n = 0.787$$

This value of C_1 agrees favorably with the value of 0.672 reported by Bays and McAdams. The value for C_2 is also similar to that reported by Borishanskiy et al. (8.7×10^{-4}), and n is almost identical to the value reported by both Kadi (0.80) and Chou (0.788).

Summary of Correlation and Discussion

The correlation recommended for thin-film forced convective shell-side boiling is:

$$h_{2\phi} = h_{conv} + \bar{h}_{NUC}$$

$$h_{conv} = h_g \exp(-0.0867 + 8{,}000\pi_2)$$

(This expression is obtained by combining Eq. 4a with the empirical relationship between ϵ and π_2. For values of π_2 that give values for the argument less than zero, the argument should be set equal to zero.)

$$h_g = 0.886\left(\frac{2k_L^2\rho_L^{4/3}g^{2/3}C_{PL}}{\pi D_T \mu_L^{1/3}}\right)^{1/3}\left(\frac{\mu_L}{\mu_w}\right)^{1/4}\left(\frac{2\,G(1-x)\,S_W}{\mu_L}\right)^{1/9}$$

$$Nu_{NUC} = 8.0\times 10^{-4}\,Pe_*^{0.787}\,Kp^{0.7},$$

or if terms are collected

$$\bar{h}_{\rm NUC} = 2.89\times 10^{-15}\left(\frac{g_c}{g}\right)^{1.143}\cdot\left(\frac{k_L^{1.0}\,P^{3.286}}{(\rho_L-\rho_v)^{1.143}\,\sigma^{2.142}}\right)\cdot\left(\frac{\rho_L C_{PL}}{\rho_V h_{fg}}\right)^{3.695}(S\Delta T_s)^{3.695}$$

(If a successful correlation is known for the specific system of interest, h_{NUC} can be directly evaluated from the empirical data. However, it is important that these data be obtained under constant wall-temperature conditions. If pool boiling experiments are carred out with heated tubes, circumferential variations in the heat transfer coefficient can cause variations in the wall temperature. Since nucleate boiling coefficients are dependent upon the local wall superheat, direct data reduction of the average heat transfer coefficient vs. average wall superheat can be misleading.)

$$\pi_2 = \left(\frac{\Delta P_{2\phi}}{g_c\rho_L}\right)^{1/2}\frac{\mu_V}{\sigma}$$

$$S = \frac{k_L}{h_{conv}X_o}\left[1-\exp\left(-\frac{h_{conv}X_o}{k_L}\right)\right]$$

$$X_o = 0.041\left[\frac{g_c\sigma}{g(\rho_L-\rho_V)}\right]^{1/2}$$

The recommended correlation for the two-phase pressure drop for in-line tubes is,

$$\Delta P_{2\phi} = \Delta P_{VT} f_D\left[\frac{1-\alpha_s}{\frac{\rho_V}{\rho_L}(Re_{VT})^{0.2}}\right]$$

where

$$f_D\left[\frac{1-\alpha_s}{\frac{\rho_V}{\rho_L}(Re_{VT})^{0.2}}\right]$$

can be obtained from Figure 5. (For staggered tubes, Diehl [1957] reports a slightly different relationship for the two-phase enhancement of pressure drop.)

$$\Delta P_{VT} = 4f_{VT}\frac{\rho_V V_{max}^2}{2g_c}$$

where f_{VT} is obtained from existing single-phase shell-side pressure drop correlations such as those of Grimison (1937). All of the above equations are dimensionally consistent.

In Figure 7, the experimental heat flux is plotted vs. the calculated value using the experimental superheat. The heat flux ranged over two orders of magnitude. The mean error is 9.5% and the average error is 0.5%.

This correlation is based on data for down-flow of both liquid and vapor. However, for down-flow liquid and up-flow vapor, the liquid film would tend to be thicker due to vapor shear but thinner due to entrainment because of the increased velocity difference between the down-flowing liquid and up-flowing vapor. Since these effects would tend to counteract each other, this proposed correlation may be reasonable for downward liquid flow and upward vapor flow.

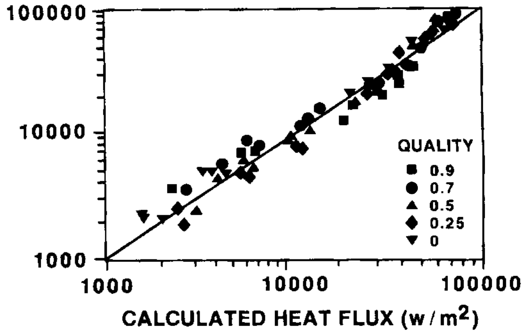

Figure 7. Experimental vs. calculated heat flux.

Acknowledgment

The authors wish to thank H. J. Grimm for his assistance in preparing the figures and K. B. Wilson for his critical review of this paper. The authors also wish to thank Desiree Pizzuto for her careful preparation of the manuscript.

Notation

Cp_L = specific heat of liquid
D_T = external diameter of horizontal tube
$f_D[\ ]$ = functional relationship as determined by Diehl (1957)
f_{VT} = friction factor, in Eq. 1
G = total mass flux, using S_w
g = acceleration due to gravity
g_c = constant required by Newton's equation
h_{conv} = portion of total heat transfer coefficient attributable to convective boiling
h_{fg} = latent heat of vaporization
h_g = heat transfer coefficient for liquid flowing over tube under conditions of zero vapor flow
$\bar{h}_{PB}$ = heat transfer coefficient during pool boiling
$\bar{h}_{NUC}$ = portion of total heat transfer coefficient attributable to nucleate boiling
$h_{2\phi}$ = sum of h_{conv} and h_{NUC}
K_p = dimensionless grouping, Borishanskiy et al. (1963)
$K_{2\phi}$ = two-phase head loss coefficient for flow past a row of tubes
k_L = thermal conductivity of liquid
Nu_B = pool boiling Nusselt number, Borishanskiy et al. (1963)

Nu_{NUC} = nucleate boiling Nusselt number for thin-film down-flow boiling
P = absolute pressure
Pe = dimensionless grouping, Borishanskiy et al. (1963)
Pe_* = modified Pe for nucleate boling during thin-film down-flow boiling
$\Delta P_{2\phi}$ = two-phase pressure drop per tube row
$\Delta P_{V only}$ = vapor pressure drop per tube row calculated for vapor flux
ΔP_{VT} = vapor pressure drop per tube row calculated using total mass flux as vapor
Re_{VT} = vapor Reynolds number using total mass as vapor, flowing through minimum area and using tube diameter as characteristic dimension
S = ratio of effective wall superheat to actual wall superheat during convective boiling
S_w = minimum distance between neighboring tubes
ΔT_s = wall superheat, wall temperature minus saturation temperature at local pressure
$V_{VT max}$ = vapor velocity using total mass as vapor, calculated using minimum flow area
$V_{V max}$ = vapor velocity using minimum flow area
x = vapor quality, ratio of vapor mass flux to total mass flux
X_o = bubble growth region, Bennett et al. (1980)

Greek letters

α_s = no-slip void fraction, $1 - \alpha_s = 1/\{[x\rho_L/(1 - x)\rho_V] + 1\}$
Γ = liquid mass flow rate per wetted length
δ_g = film thickness for liquid-only flow assuming steady state conduction
δ_{conv} = film thickness for two-phase flow assuming steady state conduction
ϵ = apparent fraction of liquid entrained in vapor core
π_1 = dimensionless parameter, Eq. 5a
π_2 = dimensionless parameter, Eq. 5b
ρ_L = liquid density
ρ_V = vapor density
σ = surface tension
μ_L = viscosity of liquid
μ_V = viscosity of vapor
μ_w = viscosity of liquid at wall conditions

Literature cited

Bays, G. S., Jr., and W. H. McAdams, "Heat Transfer Coefficients in Falling Film Heaters," *Ind. Eng. Chem.*, p. 1240 (Nov., 1937).

Bennett, D. L., M. W. Davis, and B. L. Hertzler, "The Suppression of Saturated Nucleate Boiling by Forced Convective Flow," *AIChE Symp. Ser. No. 199*, **76**, 91 (1980).

Borishanskiy, V. M., and F. P. Minchenko, as referenced in Kutateladze, S. S., ed., "Fundamentals of Heat Transfer," Academic Press, New York, p. 362 (1963). Also referenced in Hetsroni, G., "Handbook of Multiphase Systems," Hemisphere Publishing Corporation, p. 6 (1982).

Chen, J. C., "Correlation for Boiling Heat Transfer to Saturated Fluids in Convective Flow," *Ind. Eng. Chem. Des. Dev.*, **5**(3), 322 (1966).

Chou, S., "Investigation of Mass Diffusion Effects on Pool Boiling of Binary Mixtures," Ph.D. Diss., Dept. Mechanical Engineering and Mechanics, Lehigh Univ., Bethlehem, PA (1975).

Diehl, E., "Calculate Condenser Pressure Drop," *Petroleum Refiner*, p. 174 (Oct., 1957).

Grimison, E. D., "Correlation and Utilization of New Data on Flow Resistance and Heat Transfer for Cross Flow of Gases over Tube Banks," *Trans. Am. Soc. Mech. Engrs.*, **59**, 583 (1937).

Ishihara, K., J. W. Palen, and J. Taborek, "Critical Review of Correlations for Predicting Two-Phase Flow Pressure Drop Across Tube Banks," *Heat Trans. Eng.*, **1**(3), 23 (1980).

Kadi, F., "Nucleate Boiling of a Binary Mixture—Convective Boiling and Pool Boiling from a Horizontal Cylinder," Ph.D. Diss., Dept. Mechanical Engineering and Mechanics, Lehigh Univ., Bethlehem, PA (1975).

Wallis, G. B., *Int. J. Heat Mass Trans.*, **11**, 783 (1968).

Manuscript received Jan. 24, 1985, and revision received Feb. 3, 1986.